Developmental Cell, Vol. 9, 271–281, August, 2005, Copyright ©2005 by Elsevier Inc. DOI 10.1016/j.devcel.2005.07.004

Drosophila Melted Modulates FOXO and TOR Activity

Aurelio A. Teleman,[1] Ya-Wen Chen,[1] and Stephen M. Cohen*
European Molecular Biology Laboratory
Meyerhofstrasse 1
69117 Heidelberg
Germany

Summary

The insulin/PI3K signaling pathway controls both tissue growth and metabolism. Here, we identify Melted as a new modulator of this pathway in *Drosophila*. Melted interacts with both Tsc1 and FOXO and can recruit these proteins to the cell membrane. We provide evidence that in the *melted* mutant, TOR activity is reduced and FOXO is activated. The *melted* mutant condition mimics the effects of nutrient deprivation in a normal animal, producing an animal with 40% less fat than normal.

Introduction

The insulin/PI3K signal-transduction pathway controls tissue growth and metabolism in *Drosophila* and in mammals. It acts via a series of protein relocalization and phosphorylation events to relay information from the cell's environment—including growth-factor levels and nutrient availability—into the cell where it controls gene expression (via FOXO) and protein translation (via TOR). Stimulation of the insulin receptor activates PI3K, which increases the level of phosphoinositol (3, 4, 5) triphosphate (PIP3) at the plasma membrane. PIP3 binding recruits the protein kinase Akt to the membrane, where it is activated through phosphorylation by PDK1. Insulin-regulated Akt acts through two effector pathways: winged helix-Forkhead family transcription factors and the protein kinase TOR. TOR regulates the translational machinery of the cell via two well-characterized effectors: S6K and 4E binding protein (4E-BP) (Hay and Sonenberg, 2004). S6K controls ribosome biogenesis and, thus, the biosynthetic capacity of the cell. 4E-BP binds to the translation factor eIF4E and prevents assembly of a protein complex that facilitates recruitment of the ribosome.

In addition to mediating insulin-responsiveness, the TOR pathway also integrates information on cellular nutritional status and stress from the heterodimeric Tsc1/2 complex. Tsc2 serves as a GTPase-activating protein that inactivates Rheb and, thereby, reduces TOR activity (Saucedo et al., 2003; Stocker et al., 2003; Zhang et al., 2003). Tsc1/2 mutations result in TOR hyperactivation and tissue overgrowth (Gao and Pan, 2001; Potter et al., 2001; Tapon et al., 2001). Mutants in mouse Tsc1 or Tsc2 have benign overgrowths called harmatomas and show increased susceptibility to tumor formation (Kwiatkowski, 2003). Cellular AMP levels are sensed by AMP-activated protein kinase (AMPK) which phosphorylates and activates Tsc2 to inhibit TOR (Inoki et al., 2003). TOR activity is also regulated by oxygen, through the hypoxia-induced transcription factor, HIF. HIF controls expression of REDD1/Scylla/Charybdis, which reduce Tsc1/2 activity (Brugarolas et al., 2004; Reiling and Hafen, 2004).

Mutations in the core components of the pathway—the insulin receptor (InR), phosphoinositide-3-kinase (PI3K), PDK1, Akt/PKB, tuberous sclerosis complex (Tsc1/Tsc2), Rheb, the target of rapamycin (TOR), and ribosomal protein S6 kinase (S6K)—all cause tissue growth abnormalities or lethality (Hafen, 2004). A considerable body of evidence indicates that the PI3K pathway controls metabolism as well as tissue growth. Flies and mice with reduced InR/IGF receptor and PI3K activity are small and have elevated fat levels (Baker et al., 1993; Bšhni et al., 1999; Brogiolo et al., 2001; Ikeya et al., 2002; Withers et al., 1998). Mice mutant for Akt2 become insulin resistant and develop lipoatrophy as they age (Cho et al., 2001). Humans mutant for Akt2 also have abnormal metabolism and are 35% leaner than average (George et al., 2004). One output branch of the core pathway is via Foxo transcription factors. In response to insulin, Akt phosphorylates Foxo proteins, which promotes their interaction with 14-3-3 proteins and leads to cytoplasmic retention and inactivation (Brunet et al., 1999; Junger et al., 2003; Kops et al., 1999; Wolfrum et al., 2003). Foxo transcription factors have been implicated in the control of fat metabolism and lifespan in *C. elegans*, flies, and mice (Accili and Arden, 2004). The TOR branch of the pathway is also beginning to be implicated in fat metabolism. TOR phosphorylates and regulates S6K and 4E-BP. S6K mutant mice are resistant to diet induced obesity (Um et al., 2004). 4E-BP1 mutant mice have a defect in fat metabolism (Tsukiyama-Kohara et al., 2001). 4E-BP also controls fat metabolism in the fly (Teleman et al., 2005; Tettweiler et al., 2005). Recent studies have identified the eIF4E kinase LK6 as a modulator of growth and fat metabolism (Arquier et al., 2005; Reiling et al., 2005).

Here, we report the identification of a novel modulator of the insulin/PI3K pathway, Melted. The *melted* gene encodes a PH domain protein that interacts with both Tsc1 and FOXO. Melted protein can recruit the Tsc1/2 complex to the cell membrane and thereby modulate its output via the TOR pathway. Melted can also recruit FOXO to the membrane in an insulin-regulated manner and thereby influence expression of FOXO targets. By reducing TOR activity and at the same time increasing FOXO activity, the *melted* mutant mimics the effects of nutrient deprivation in a normal animal, producing a lean phenotype.

Results

Melted Modulates Tissue Growth

Melted was identified in a gain-of-function screen for genes affecting tissue growth during *Drosophila* devel-

*Correspondence: cohen@embl.de
[1]These authors contributed equally to this work.

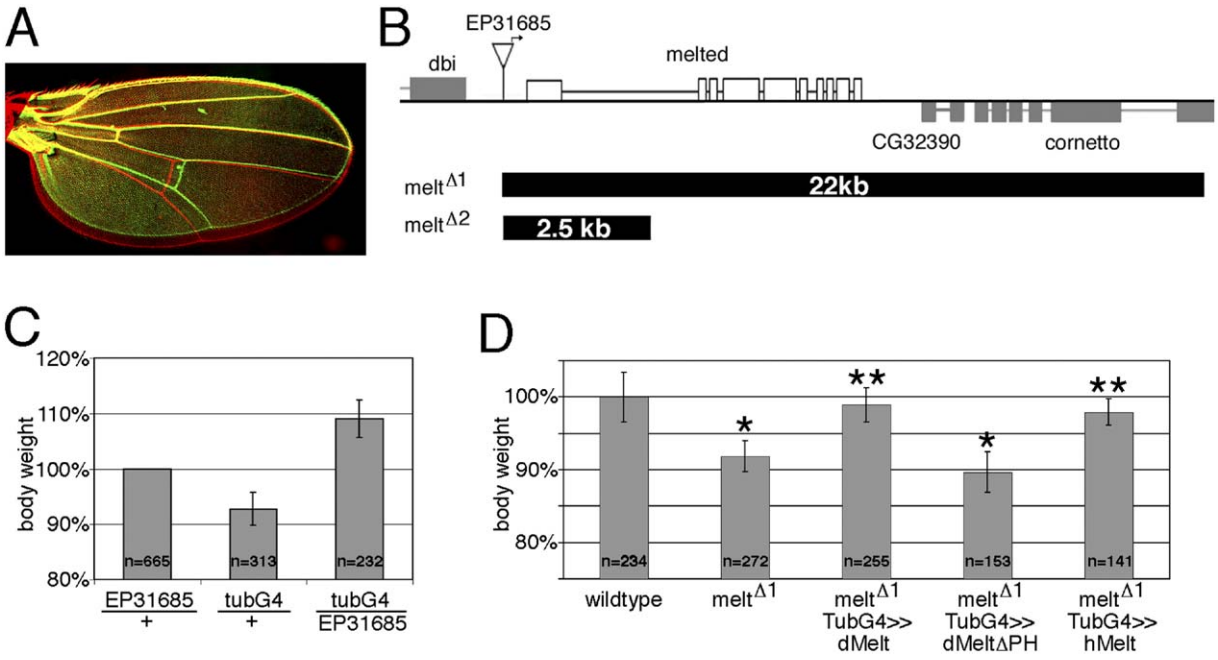

Figure 1. The *melted* Gene Product Regulates Tissue Growth

(A) Overexpression of *melted* in the posterior compartment (red wing; *engrailed-gal4, EP31685*). A normal wing is shown in green for comparison. Note that the anterior compartments are the same size (overlap) but the posterior (lower) is larger in the red wing.

(B) Schematic representation of the *melted* locus. $melt^{\Delta 1}$ is a 22-kb deletion, including the adjacent genes *CG32390* and *cornetto*. $melt^{\Delta 2}$ deleted 2.5 kb of DNA, including exon 1. The first exon of the predicted gene is noncoding, with the ATG for the open-reading frame located in exon 2. RT-PCR of exons 5–7 showed that an alternate form of *melt* transcript was produced in the homozygous $melt^{\Delta 2}$ deletion flies, suggesting that it is not a null allele.

(C) Average body weight of 3-day-old wild-type male flies, *tubulin-GAL4* flies, and flies overexpressing *EP31685.* n = number of flies measured. Error bars represent standard deviation.

(D) Average body weight of 3-day-old wild-type male flies, $melt^{\Delta 1}$ homozygous deletion mutant flies, and $melt^{\Delta 1}$ homozygous mutants expressing full-length *Drosophila* Melted (dmelt), dMelt lacking the PH domain (dMeltDPH), or the full-length human Melted (hMelt). In addition, eggs laid by $melt^{\Delta 1}$ homozygous females were 13% smaller than control eggs (t test = 10^{-7}; rescued by expression of *UAS-melt*). Asterisk indicates statistically significant difference from wild-type. Double asterisks indicates statistically significant difference from $melt^{\Delta 1}$.

opment. EP31685 caused overgrowth when expressed in the posterior half of the wing with *en-GAL4* (Figure 1A, the red wing expressed EP31685). When expressed ubiquitously with *tubulin-GAL4*, EP31685 caused a small but statistically significant increase in total body weight (Student's t test < 0.005) (Figure 1C). EP31685 is located ~50 bp upstream of the annotated gene *melted* (*melt*, CG8624) (Figure 1B). Using a *UAS-melt* transgene, we verified that the *melted* transcription unit is responsible for the tissue overgrowth phenotype (not shown).

Deletions were prepared with P-element-mediated male recombination (Preston and Engels, 1996) starting from EP31685 (Figure 1B) to generate *melted* mutants. $melt^{\Delta 1}$ is a 22-kb deletion that removes the entire *melted* gene and two adjacent genes. The second allele, $melt^{\Delta 2}$ is a 2.5-kb deletion that removes the first exon of CG8624. Flies homozygous mutant for $melt^{\Delta 1}$ were semiviable (70% viable to adult) and fertile but were ~10% smaller than control flies (Figure 1D). Though small in magnitude, the reduction in body size was statistically significant (t test < 0.005). Flies heterozygous mutant for $melt^{\Delta 1}/melt^{\Delta 2}$ were also significantly smaller than control flies (not shown). Two additional lines of evidence indicate that the growth defect was due to loss of *melted* and not the other genes deleted in $melt^{\Delta 1}$. First, the growth defect of the homozygous $melt^{\Delta 1}$ deletion flies was fully rescued by ubiquitous expression of the *UAS-melt* transgene (Figure 1D). Second, flies expressing UAS-RNAi constructs directed against two different regions of the *melt* transcript caused tissue undergrowth, resembling the $melt^{\Delta 1}$ phenotype (not shown).

The predicted Melted protein is conserved in *C. elegans* (CE25943), mice (Muto et al., 2004), and humans (HGNC, KIAA1692). Alignment of these sequences showed a conserved region at the N terminus (76% similar in fly and human) and a conserved Pleckstrin Homology (PH) domain at the C terminus. Ubiquitous expression of Melted lacking the PH domain did not rescue the $melt^{\Delta 1}$ size defect (Figure 1D), indicating that the PH domain is required for Melted function. The truncated protein is likely to fold correctly because it was used successfully as bait in a yeast two-hybrid screen to detect proteins that also interact with full-length Melted (see below). The human homolog of Melted also

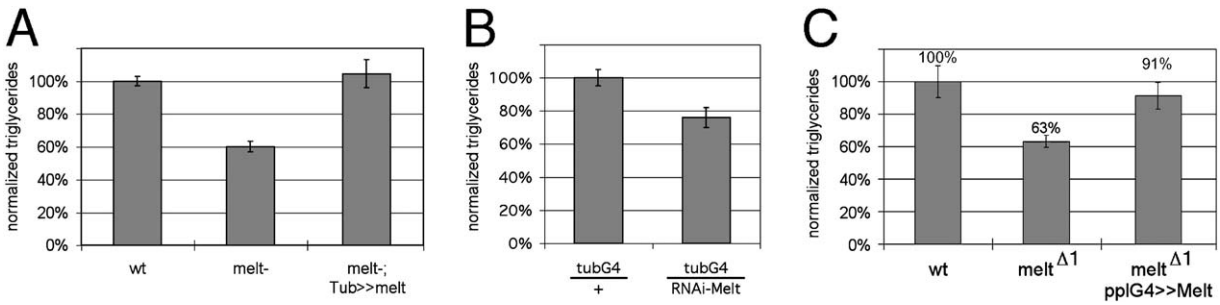

Figure 2. Reduced Fat Reserves in *melted* Mutants

(A) Total body fat (normalized to total protein) in wild-type, $melt^{\Delta 1}$, and $melt^{\Delta 1}$ male flies rescued by expression of full-length Melted. Error bars represent standard deviation (three replicates).

(B) Total body fat in male flies expressing UAS-melted-RNAi.

(C) Normalized total body fat of adult males of indicated genotypes.

rescued the size reduction of the $melt^{\Delta 1}$ mutant (Figure 1D), indicating that the molecular function of Melted is conserved.

melted Mutants Are Lean

We next asked whether Melted might also affect fat metabolism. *Drosophila* stores fat mainly as triglycerides. Total body triglyceride was measured for $melt^{\Delta 1}$ mutant and control flies reared under identical controlled conditions. When normalized to total protein to take into account the 10% reduced body size of *melted* mutants, *melt* mutant flies had only 60% as much triglyceride as control flies. This reduction in fat content was statistically significant (t test < 0.001) and was rescued by ubiquitous expression of a *UAS-melt* transgene (Figure 2A). Further confirmation that the leanness of the mutant was due to reduced *melted* expression was obtained by ubiquitous expression of a *melted* UAS-RNAi construct in flies (25% leaner) (Figure 2B). Total body triglycerides of wandering third instar $melt^{\Delta 1}$ mutant larvae were also 20% lower than controls, indicating that Melted regulates fat levels throughout development as well as in the adult (not shown).

Fat levels can be controlled by humoral factors, including adipokinetic hormone (AKH), which induces mobilization of fat reserves (Lee and Park, 2004). Insulin-like peptides (ILPs) also control fat metabolism in the fly (Ikeya et al., 2002 Hwangbo et al., 2004). To determine whether elevated AKH or ILP-2, -3, and -5 expression could explain the leanness of *melted* mutants, we tested transcript levels by quantitative RT-PCR. Transcript levels were not significantly elevated. Because altered expression of the known humoral regulators did not provide an explanation for the mutant phenotype, we asked if there was a defect in adipose tissue. The "fat body" is the main fat-storage organ of the fly, containing over 80% of total body triglycerides. We isolated $melt^{\Delta 1}$ mutant and control fat body tissue from larvae and found 25% lower triglyceride level in the mutant tissue. The total body leanness of $melt^{\Delta 1}$ mutants was rescued by expressing *melted* specifically in the fat body with *ppl-GAL4* (Figure 2C). In contrast, expression of *melted* in the nervous system with *elav-GAL4* or in brain neurosecretory cells with *dILP3-GAL4* did not rescue the mutant (not shown). This indicates that Melted activity is required in adipose tissue.

Membrane Localization via the Melted PH Domain

Melted contains a C-terminal PH domain. We tested if bacterially expressed Melted protein binds to immobilized phosphoinositides. At higher concentration, Melted bound many phosphoinositides but at lower concentrations, showed preferential binding to PI(5)P (Figures 3A and 3A′). The PH domain of Melted expressed as a GST fusion exhibited a similar binding pattern, although with reduced selectivity. Although Melted did not show strong binding to PIP3 in vitro, we generated a GFP fusion to the PH domain (MeltPH-GFP) and tested it in S2 cells for insulin-induced relocalization. MeltPH-GFP was detectable predominantly at the cell membrane when cells were serum-starved to deprive them of insulin and after insulin-stimulation without apparent difference (Figures 3B and 3B′). The MeltPH-GFP fusion was also predominantly cortical in wing imaginal disc cells, whereas a Melted-GFP fusion protein lacking the PH domain was cytoplasmic (Figures 3C and 3D), suggesting that the majority of Melted protein is localized to the membrane under normal conditions. This was confirmed by subcellular fractionation of wing-disc cells. The majority of the endogenous Melted protein was recovered in the membrane fraction, with a lesser amount in the cytoplasm (Figure 3E). No signal was detected in corresponding fractions prepared from *melted* mutant tissue, confirming the specificity of the antibody. Control proteins fractionated predominantly as cytoplasmic (Y14) or membrane-associated (PVR). These results suggest that the endogenous Melted protein is membrane localized via its PH domain and that its localization is not regulated by insulin-dependent changes in PIP3 levels. The PH domain is required for Melted function in vivo (Figure 1D).

Melted Protein Binds to Tsc1 and Modulates TOR Activity

To study the function of the N-terminal domain, we performed a yeast two-hybrid screen with MeltDPH as bait

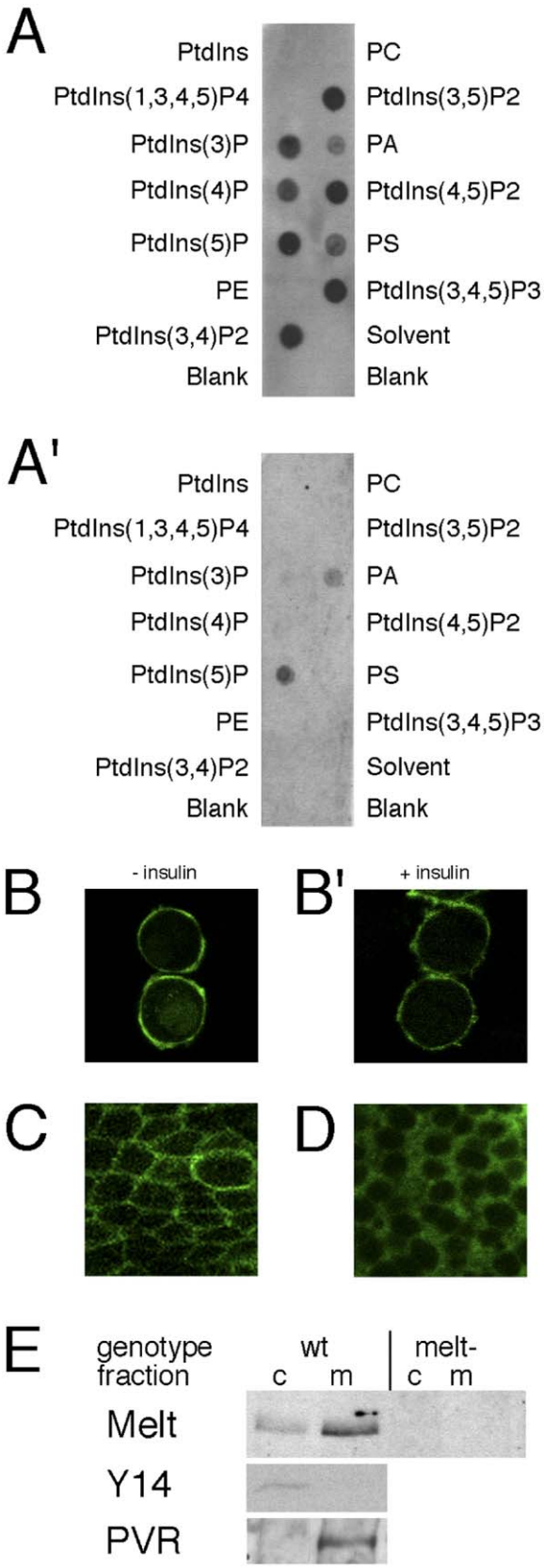

to screen 2.7 million clones from a larval cDNA library. Six interacting genes were isolated: Tsc1 (four independent clones), 14-3-3e (three independent clones), CG16719, CG5171, CG6767, and CG8242 (one each). When expressed in S2 cells by cotransfection, Melted coimmunoprecipitated with Myc-tagged Tsc1. Interaction of Melted and Tsc1 in S2 cells was also visualized by immunofluorescence microscopy. Tsc1myc was uniformly distributed in the cytoplasm when expressed alone (Figure 4A, row 1; S2 cells lack endogenous Melted). Coexpression with Melted caused Tsc1-myc to shift predominantly to the cell membrane (Figure 4A, row 2). When expressed in S2 cells, Tsc2 was uniformly distributed in the cytoplasm (Figure 4A, row 3). Coexpression of Tsc2 with Melted did not cause a relocalization of Tsc2 to the membrane, suggesting that Melted and Tsc2 do not interact directly (Figure 4A, row 4). However, when coexpressed with Melted and Tsc1, Tsc2 also relocated (Figure 4A, row 6), indicating that Melted can recruit the Tsc1/2 complex to the cell membrane.

Does this interaction affect TOR pathway activity? Previous reports have shown that increased PI3K or TOR signaling in the adipose tissue increased fat accumulation or reduced fat consumption (autophagy) (Britton et al., 2002; Rusten et al., 2004). The observation that *melted* mutants are lean, could be explained if TOR activity is reduced in the mutant. To test this more directly, we assayed the level of TOR-dependent phosphorylation of 4E-BP in control and $melt^{\Delta 1}$ mutant fat bodies (Figure 4B). Phosphorylation of *Drosophila* 4E-BP at positions 36/47 depends on TOR activity and can be visualized with an antibody specific to the corresponding phosphorylated peptide from human 4E-BP (Miron et al., 2001). Although the total level of 4E-BP protein was higher in $melt^{\Delta 1}$ mutant tissue, the level of phosphorylation was not correspondingly elevated (perhaps mildly reduced) (Figure 4B, left). The increase in total 4E-BP level reflects a 2- to 3-fold increase in transcript levels in the mutant fat body (Figure 4C). We increased 4E-BP levels by a comparable amount in wild-type fat body, as a control, with *ppl-Gal4 UAS-4E-BP* and observed that the level of 4E-BP phosphoryla-

Figure 3. Membrane Localization of Melted, a PIP Binding Protein

(A and A′) Immunoblots showing binding of bacterially expressed Melted protein to immobilized phosphoinositides (PIP Strip, Echelon Biosciences) at Melted protein concentrations of roughly 100 ng/ml (A) or 10 ng/ml (A′). PtdIns, phosphatidylinositol; PE, phosphatidylethanolamine; PC, phosphatidylcholine; PS, phosphatidylserine; PA, phosphatidic acid. The binding pattern for a control with the PIP3 binding domain of GRP1 was different.

(B) Immunofluorescence showing membrane localization of Melted-GFP in serum starved (–insulin) and insulin-treated S2 cells.

(C) Immunofluorescence showing membrane localization of MeltedPH-GFP in wing-imaginal disc cells.

(D) Immunofluorescence showing cytoplasmic localization of Melted-GFP lacking the PH domain (MeltDPH-GFP) in wing-imaginal disc cells.

(E) Immunoblot showing the distribution of Melted protein in cytosolic (c) and membrane (m) fractions of wild-type and $melt^{\Delta 2}$ homozygous mutant tissue. Controls are anti-Y14, a cytoplasmic protein (Hachet and Ephrussi, 2001), and anti-PVR (PDGF/VEGF receptor a transmembrane protein) (Duchek et al., 2001).

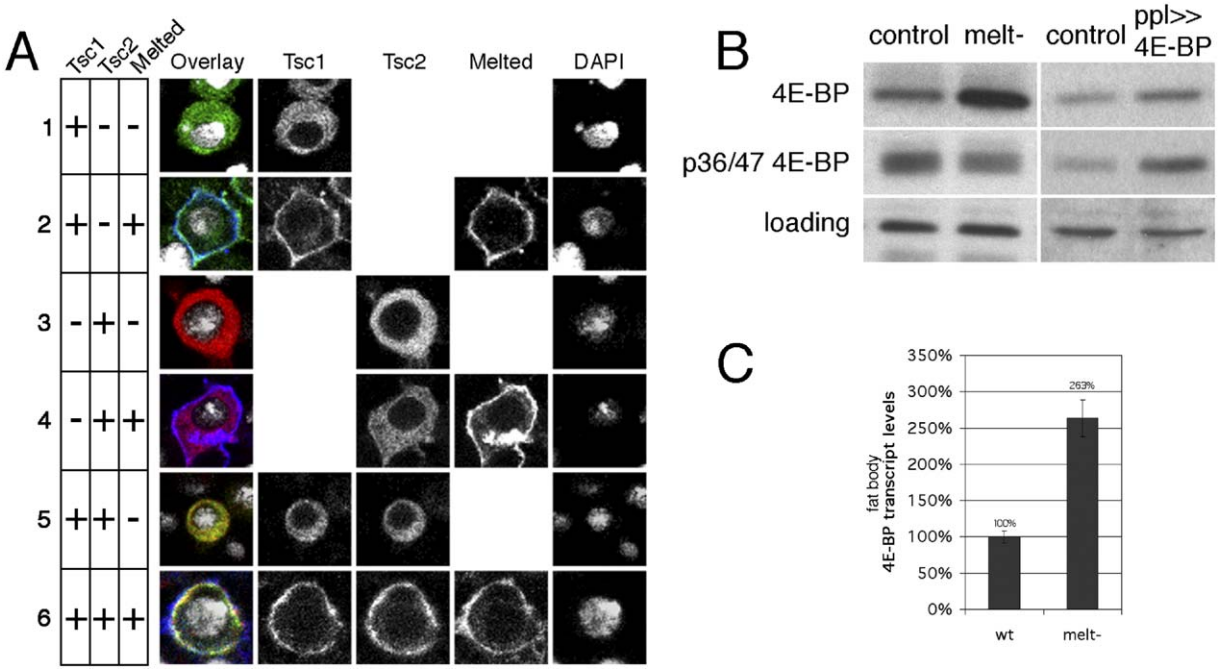

Figure 4. Melted Binds Tsc1/2 and Regulates TOR Activity

(A) Immunofluorescence showing S2 cells transfected to express Tsc1, Tsc2, and Melted, as indicated. Tsc1 was epitope tagged with myc (green), and Tsc2 was tagged with V5 (red). Melted was detected with anti-Melted antibody (blue). Nuclei were visualized with DAPI (white).

(B) Left, immunoblot of fat-body tissue from wild-type and *melt* mutant larvae. Right, immunoblot of fat-body tissue from wild-type and larvae expressing 4E-BP under ppl-Gal4 control. Upper panels, probed with anti-4E-BP to visualize total 4E-BP protein. Middle panels, probed with phosphospecific antibody to visualize 4E-BP protein phosphorylated on Thr36/47. Lower panels, loading controls.

(C) Quantitative RT-PCR comparing 4E-BP transcript levels in wild-type and *melt* mutant fat-body tissue. Error bars represent standard deviation.

tion was correspondingly elevated (Figure 4B, right). This indicates that TOR activity is not limiting in wild-type fat body. Thus, the observation that 4E-BP phosphorylation did not increase, despite increased total 4E-BP, provides evidence that TOR activity is reduced in the *melted* mutant adipose tissue.

Melted Binds to FOXO and Modulates FOXO Activity

As a second means to identify possible functions of Melted, we used the Eukaryotic Linear Motif server (http://elm.eu.org/) to look for functional motifs conserved between fly and human Melted. The only conserved motifs found in the N-terminal region of these proteins were two Forkhead-associated domain ligand domains (LIG_FHA_1). Forkhead transcription factors FoxA2, FoxA3, FoxC2, and FoxO1 are involved in glucose and fat metabolism. Insulin signaling activates Akt, which phosphorylates FOXO and leads to its retention in the cytoplasm. We therefore asked if Melted affects the subcellular localization of a FOXO-GFP fusion protein. FOXO-GFP was predominantly nuclear in the absence of insulin stimulation in serum-starved S2 cells and increased in the cytoplasm after insulin stimulation (Figure 5A, rows 1 and 2). In serum-starved cells co-transfected to express Melted, FOXO-GFP was still primarily nuclear (Figure 5A, row 3), but much of the non-nuclear protein appeared at the membrane colocalized with Melted. Upon insulin stimulation, we observed a robust increase in the level of FOXO-GFP at the cell membrane (Figure 5A, row 4). The interaction was confirmed by coimmunoprecipitation of Melted with FOXO in insulin-stimulated S2 cells (Figure 5B).

The observation that insulin stimulation induced a shift toward membrane localization of FOXO in the presence of Melted in S2 cells raised the possibility that *melted* regulates FOXO activity in vivo. To address this, we examined expression of the FOXO target 4E-BP (Junger et al., 2003) in wild-type and *melted* mutant animals. Under fed conditions, insulin signaling is active and 4E-BP transcript levels are relatively low (Figure 5C). In wild-type flies that were starved for 24 hr to reduce insulin levels and thereby activate FOXO, 4E-BP transcript increased ~4-fold (Figure 5C). In starved flies lacking Melted, 4E-BP transcript increased over 25-fold. This increase in 4EBP transcription was absent in the starved melted/FOXO double mutant, confirming that it is FOXO dependent. Thus, in the absence of Melted, FOXO activity is higher than normal, suggesting that Melted limits FOXO activity in vivo.

Melted Acts via TOR and FOXO

To determine whether the elevated FOXO activity observed in *melted* mutants contributes to the lean phenotype of these animals, we compared the normalized triglyceride levels of *melted* mutant and *melted foxo* double-mutant flies. Reducing FOXO activity suppressed

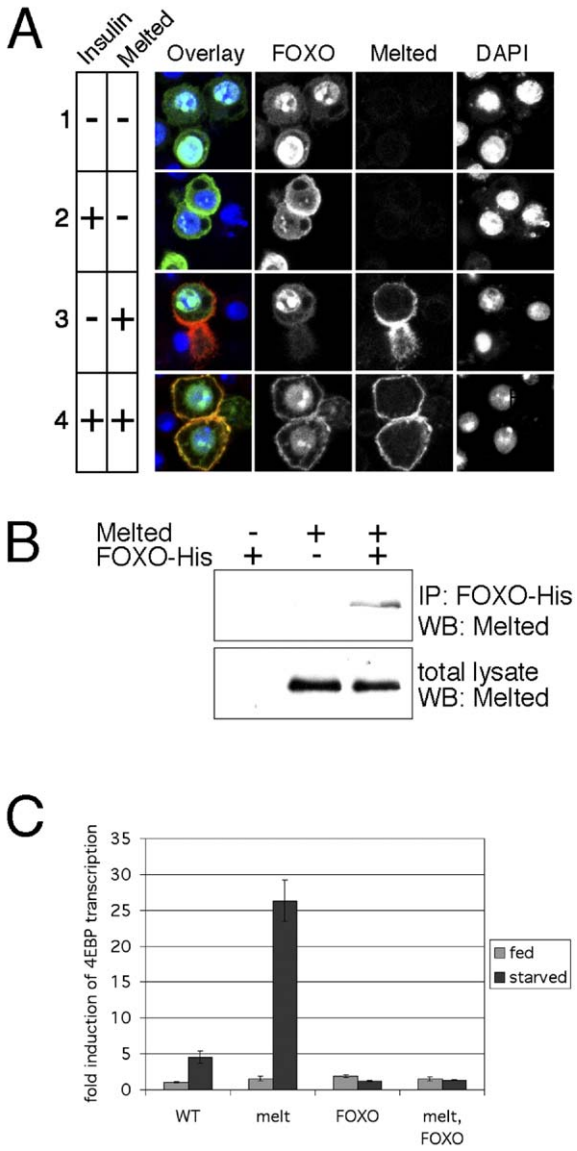

Figure 5. Melted Binds FOXO and Regulates Expression of the FOXO Target 4E-BP

(A) Immunofluorescence showing S2 cells transfected to express FOXO-GFP and Melted, as indicated. FOXO-GFP was visualized with anti-GFP (green). Melted was detected with anti-Melted antibody (red). Nuclei were visualized with DAPI (blue). Cells were treated with insulin (+) or serum starved (–) as indicated.

(B) Coimmunprecipitation of Melted with HIS-tagged FOXO. S2 cells were transfected to express FOXO-HIS and/or Melted as indicated. Lysates were immunoprecipitated with anti-HIS and blots probed with anti-Melted. Melted expression in the total lysates is shown below.

(C) Quantitative PCR comparing 4E-BP transcript levels in wild-type, *melt*, *foxo*, and *melt/foxo* double-mutant flies. Fed flies have normal levels of circulating insulin and, therefore, low FOXO activity. 4E-BP gene expression increased after starvation for 24 hr to reduce insulin levels and showed a further FOXO-dependent increase in the *melt* mutant. Error bars represent standard deviation.

the leanness of the *melted* mutant to a considerable degree, reaching near normal fat levels (Figure 6A). The rescue was highly statistically significant (t test = 10^{-5}). *foxo* mutants did not show higher-than-normal fat levels compared to wild-type (not shown). These observations suggest that Melted acts by regulating FOXO activity to control expression of genes important in fat metabolism.

melted mutants also exhibit reduced TOR activity. To determine whether TOR activity affects fat accumulation, we tested the effects of increasing TOR activity in wild-type and *melted* mutant adipose tissue. We made use of a UAS-TOR transgene that can provide TOR activity in vivo when expressed at appropriate levels (Hennig and Neufeld, 2002). We first confirmed that expression of UAS-TOR under ppl-Gal4 control in adipose tissue led to increased total body fat (Figure 6B) (t test = 0.03), as did increasing PI3K activity (not shown) (see also Britton et al., 2002). In contrast, a comparable elevation of TOR expression in *melted* mutant flies had no effect on fat levels (Figure 6C). Both this result and the significant rescue caused by removal of FOXO indicate that in the *melted* mutant, the FOXO branch of the pathway becomes limiting for fat accumulation. In view of this finding, we next asked whether elevated TOR pathway activity could increase fat levels in the *melted* mutant if FOXO activity was simultaneously reduced. To do so, we made use of the catalytic subunit of PI3K (Dp110) to inactivate FOXO and simultaneously activate TOR. The fat body driver lsp2-Gal4 or the UAS-Dp110 transgenes had little effect on their own in the *melted* mutant background, but when combined, the elevated PI3K activity in the fat body increased fat levels of the *melted* mutant (Figure 6D). The effect was stronger than that of removing FOXO only, increasing fat levels to above normal (compare Figures 6A and 6D). Taken together, these observations suggest that the TOR branch of the pathway contributes to the control of fat levels under conditions in which FOXO activity levels are low. This is normally the case in feeding animals in which insulin levels are relatively high (FOXO activity is elevated under starvation conditions: compare 4E-BP levels in fed versus starved wild-type and *foxo* mutant flies) (Figure 5C). Under conditions in which insulin levels are low or in the melted mutant, in which FOXO activity is elevated, the effects of FOXO appear to dominate.

Transcriptional Profiling of *melted* Mutant Adipose Tissue

To better understand the metabolic impact of the loss of Melted function in the adipose tissue, we performed microarray expression profiling of *melted* mutant versus control fat body. We used microarrays containing 11,445 cDNA clones (DGC1 and DGC2 collection) and analyzed the data with Statistical Analysis of Microarrays (SAM) in the MeV module of the TIGR TM4 microarray software suite (http://www.tigr.org/software/tm4/mev.html) (Tusher et al., 2001). Allowing for a 1% false-positive rate (q value < 0.01), we identified 315 genes that were upregulated and 405 genes that were downregulated in the *melted* mutant (Table S1 available with this article online). This represents 6% of all genes sampled and reflects substantial reprogramming of the transcriptional profile of the adipose tissue. Within this set, we considered genes altered by at least 1.5-fold

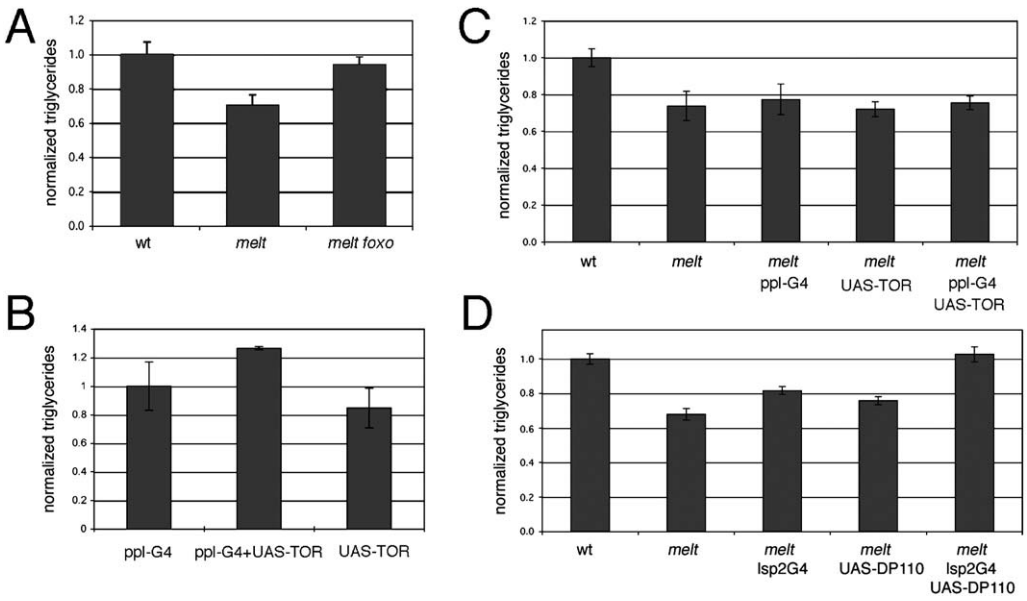

Figure 6. Melted Acts via FOXO and TOR

(A) Total body triglyceride (normalized to total protein) in wild-type, *melt*$^{\Delta 1}$, and *melt*$^{\Delta 1}$ *foxo* double-mutant 3-day-old male flies. *melt*$^{\Delta 1}$ and *melt*$^{\Delta 1}$ *foxo* double-mutant larvae were hand selected and grown without competition from heterozygous siblings. Error bars represent standard deviation (5–9 replicates each).

(B) Normalized total body triglyceride in 3-day-old male flies containing the UAS-TOR or ppl-Gal4 transgenes or both combined to express UASTOR under ppl-G4 control. Error bars represent standard deviation. One representative example is shown. The experiment was repeated five times, yielding a t test = 0.03.

(C) Normalized total body triglyceride in 3-day-old male wild-type, *melt*$^{\Delta 1}$, and *melt*$^{\Delta 1}$ mutant flies carrying the ppl-gal4 driver, UAS-TOR transgene, or expressing UAS-TOR under ppl-Gal4 control.

(D) Normalized total body triglyceride in newly enclosed wild-type, *melt*$^{\Delta 1}$, and *melt*$^{\Delta 1}$ mutant flies carrying the fat-body-specific gal4 driver lsp2, the UAS-Dp110 transgene (the catalytic subunit of PI3K), or expressing UAS-Dp110 under lsp2-Gal4 control.

(249 genes) and grouped them according to their functional annotation (http://www.flybase.org/). 46% of the regulated genes are involved in metabolism (Figure 7A). Interestingly, many of these are involved in lipid metabolism (Table S1). Ten are cytochrome P450 enzymes involved in the oxidation of lipophilic molecules. We confirmed the transcriptional regulation of some of these genes by semiquantitative RT-PCR (Table S1, second column). In addition to the genes involved in fat metabolism, a significant proportion of the misregulated metabolic genes are involved in protein degradation.

Several of the downregulated genes are involved in the accumulation of triglycerides. One of the most highly downregulated genes in the *melt*$^{\Delta 1}$ mutant adipose tissue is the transcription factor *sugarbabe* (2.4-fold). *sugarbabe* was previously identified as a gene controlling the conversion of sugars to fats (Zinke et al., 2002). It is the second most highly upregulated gene

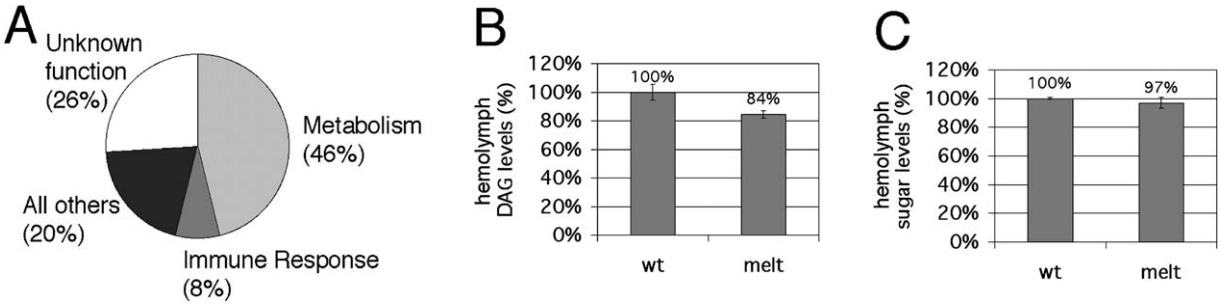

Figure 7. Transcriptional Changes in *melt*$^{\Delta 1}$ Mutant Fat Body and Resulting Metabolic Effects

(A) Pie chart showing the distribution of genes misregulated >1.5-fold in the *melt* mutant fat body.

(B) Total circulating diacylglycide levels in hemolymph from wild-type and *melt*$^{\Delta 1}$ mutant larvae. The reduction in circulating DAG is statistically significant (t test = 0.02).

(C) Total circulating sugar levels in hemolymph from wild-type and *melt*$^{\Delta 1}$ mutant larvae.

when flies were fed sugar but deprived of lipids, and it becomes expressed in the adipose tissue, gut, and malphighian tubules. Acetyl-CoA sythase (AcCoAS) was also identified in the same screen as a gene upregulated on a sugar diet (7.3-fold), whereas in the *melt*$^{\Delta 1}$ mutant adipose tissue it was downregulated (1.8-fold). The downregulation of both *sugarbabe* and AcCoAS suggests that *melt*$^{\Delta 1}$ mutant adipose tissue might not be able to accumulate enough lipid. This is corroborated by the finding that glycerol kinase (Gyk) and PEPCK are among the genes most downregulated in *melted* mutant adipose tissue (Table S1). In order to generate triglycerides, both free fatty acids and 3-phosphoglycerol are required by the cell. In vertebrate brown adipose tissue, 3-phosphoglycerol is made by Gyk, whereas in white adipose tissue, it is made by PEPCK (Hanson and Reshef, 2003). PEPCK is rate limiting in that loss of function in the mouse leads to lipodystrophy, whereas overexpression in mouse adipose tissue leads to obesity. Therefore, the finding that both Gyk and PEPCK are downregulated in the *melt*$^{\Delta 1}$ mutant fat body suggests that these animals are lean because they do not accumulate enough lipid in the adipose tissue. Consistent with what is known in vertebrates, we detected increased PEPCK levels by quantitative RT-PCR in other nonadipose tissues under starvation conditions and in the *melted* mutant; thus, the transcriptional changes in adipose and nonadipose tissues do not always correlate. Recently, adipose triglyceride lipase has been reported to catalyze the initial step in triglyceride hydrolysis in mice and inhibition of this enzyme markedly decreases total adipose acylhydrolase activity (Zimmermann et al., 2004). BLAST searches identify two *Drosophila* homologs of adipose triglyceride lipase: CG5295 and CG5560. Interestingly, CG5295 expression was markedly reduced in the *melt*$^{\Delta 1}$ mutant fat body. This suggests that lipid hydrolysis might be downregulated in the mutant adipose tissue.

To test experimentally these predictions from expression data, we measured circulating lipids, which, in the fly, are mobilized from the fat body and delivered to peripheral tissues as diacylglycerides (DAG) in the hemolymph (Canavoso et al., 2001). Hemolymph DAG was low in *melt*$^{\Delta 1}$ mutant larvae compared to controls (Figure 7B) (t test = 0.02). Thus, it is not likely that the reduced triglycerides in the adipose tissue can be explained by increased mobilization of fat in the form of circulating DAG. We also measured the level of circulating blood sugar (trehalose + glucose) and found that it was not elevated in the *melt*$^{\Delta 1}$ mutant (Figure 7C). These experiments, together with the expression data, suggest that the leanness observed in the mutant is likely due to reduced triglyceride accumulation in adipose tissue.

Discussion

Melted Functions at the Plasma Membrane

Melted contains two functional domains, identified as regions of high conservation between the fly and human proteins—an N-terminal protein interaction domain and a C-terminal PH domain. The PH domain targets Melted to the cell membrane. PH-GFP fusion proteins show sharp membrane localization, and fractionation assays showed that in steady state, the majority of endogenous Melted protein is membrane associated. Rescue assays show that unlike the full-length protein, Melted protein missing the PH domain cannot rescue the *melt*$^{\Delta 1}$ mutant phenotypes. Thus, Melted protein requires its PH domain, and presumably its membrane localization, to have biological activity in vivo.

On this basis, we propose that Melted may function as an adaptor, facilitating association of the TSC complex and FOXO with their upstream-signaling inputs. FOXO and Tsc2 are phosphorylated in vivo by Akt/PKB, which becomes activated at the cell membrane when it binds PIP3 and is phosphorylated by PDK1. Although the phosphorylation of Tsc2 by PKB is not strictly necessary for viability (Dong and Pan, 2004), it is possible this phosphorylation is modulatory in function. Tsc2 is also regulated via phosphorylation by AMPK. AMPK is membrane associated through its myristoylated β subunit. Therefore, it is plausible that recruiting the Tsc complex and FOXO to the cell membrane might alter their state of activation. We consider it unlikely that Melted could sequester the TSC complex and FOXO proteins at the membrane. Instead, an intriguing possibility is that by transiently binding these proteins, Melted could facilitate their phosphorylation.

Reduced FOXO phosphorylation is expected to increase FOXO activity, and indeed we found (1) upregulation of the FOXO target 4E-BP (Junger et al., 2003; Puig et al., 2003) in the *melted* mutant and (2) that reduced FOXO levels could suppress the fat-accumulation defect in the *melted* mutant. These observations indicate that FOXO activity is increased in the *melted* mutant. Similarly, reduced Tsc2 phosphorylation is expected to lead to increased Tsc2 activity and, thus, reduced TOR activity. Indeed, we found that TOR activity becomes limiting for 4E-BP phosphorylation in the *melted* mutant.

FOXO, TOR, and Metabolism

melt$^{\Delta 1}$ mutant animals are lean because of lower lipid levels in adipose tissue. This phenotype is autonomous to the fat body because it can be rescued by tissue-specific expression of Melted. We have presented evidence that elevated FOXO activity in the mutant is important in this context. Adipose tissue undergoes a dramatic transcriptional change upon loss of *melted* function. At the 99% confidence level, 249 genes were misregulated by more than 1.5-fold in the fat body. 63% of the misregulated genes for which a function is annotated are metabolism related. Although many of these are involved in lipid or carbohydrate metabolism, we were surprised to find a significant number of genes involved in proteolysis and amino acid metabolism. Recently, FOXO has been shown to promote protein turnover during fasting (Sandri et al., 2004).

Members of the TOR signaling pathway have been implicated in the control of fat metabolism in flies and mice. Both S6K and 4E-BP mutant mice are either lean or resistant to diet-induced obesity (Um et al., 2004, Tsukiyama-Kohara et al., 2001). Likewise, 4E-BP mutant flies show increased sensitivity to nutrient depriva-

tion, leading to abnormal fat loss (Teleman et al., 2005). In the fly, we find that activation of the TOR pathway in the fat body promotes fat accumulation. Because TOR activity is reduced in the *melted* mutant fat body, we believe this contributes to the observed leanness. This is supported by the fact that inactivating FOXO in the melted mutant leads to a 90% rescue, whereas simultaneously inactivating FOXO and restoring TOR function (via PI3K) has a more pronounced effect, elevating fat levels to above normal. When the animal is under conditions of limited nutrition, in which FOXO activity is high, the effects of FOXO-dependent transcription appear to dominate and shift the animal to a mode of net fat consumption. When the animal is under normal fed conditions, the ability of TOR to serve as a sensor of cellular nutritional status may be important in controlling fat accumulation.

The effect of Melted on both tissue growth and metabolism is modulatory. In the absence of Melted protein, both tissue growth and lipid metabolism function, although with modified characteristics. The magnitude of the effect caused by Melted overexpression is smaller than that caused by Tsc1/2 loss of function. This phenotype is similar to those of other components of the PI3K/TOR pathways that have recently been studied in flies. For instance, FOXO mutant flies have no detectable growth abnormalities and are impaired in their response to oxidative stress (Junger et al., 2003). We tested whether *melt*$^{\Delta 1}$ mutant flies are also sensitive to oxidative stress by feeding them food with H_2O_2, and indeed they are. *Scylla* and *Charybdis* are two genes upstream of the Tsc1/2 complex that regulate S6K activity. Scylla and Charybdis double-mutant flies show very mild growth defects but are impaired in their response to hypoxia and have abnormal lipid levels (Reiling and Hafen, 2004). Lk6 kinase, like 4E-BP, regulates eIF4E activity. Lk6 mutant flies are 20% smaller than controls and contain elevated lipid levels (Arquier et al., 2005; Reiling et al., 2005). Thus, the TOR pathway appears to be closely regulated by several modulators, Melted being a new member of this group.

Melted is highly conserved between flies and mammals, and human Melted expression rescues the mutant fly phenotype. In view of the overall similarity in the biochemistry and biological functions of the insulin/PI3K pathway in flies and mammals, the possibility that Melted might have a comparable role in mammalian metabolism merits consideration.

Experimental Procedures

Plasmids

A full-length Melted cDNA was cloned into pUAST as an EcoRI-NotI (pAT159). This clone differs from the annotated CG8624 because of splicing differences. Human Melted was cloned by RT-PCR from HeLa cell cDNA and cloned into pUAST (pAT206). The dMeltPH-GFP fusion was constructed by amplifying the PH domain ccc cctcgagGCTTTCTCAATGGCAGCAAT, cgcggatcctaCGTGGGATTA TCTCGGGCCTG for cloning into a metallothionine promoter vector containing GFP (pAT195). The GFP fusion was then cloned into pUAST (pAT202) for transformation of *Drosophila*. His-tagged Melted was made by inserting the dMelt ORF into pET23a (plasmid pAT160). For the yeast two-hybrid screen, a bait plasmid containing dMelt without the PH domain was made by inserting a 1695-bp EcoRI-XhoI fragment from pAT159 into the EcoRI-SalI sites of pGBDU (pAT165). Myc-tagged Tsc1 and of V5/His-tagged Tsc2 plasmids were a kind gift of Duojia Pan. FOXO-GFP was constructed as a C-terminal GFP fusion in pUAST. Two UAS-melted-RNAi transgenes were prepared by PCR (tctagaCTCGCACGCG GACTATGTGAA and tctagaCTTGGCATGGGGTGGCTCTTC; tctag aCGCCCACACGTTGCAGCATTG and tctagaGGACTCCCGCGTGC TAAG) and cloned into pWIZ (Lee and Carthew, 2003).

Strains and Transgenic Lines

engrailed-Gal4 and tubulin-Gal4 are described in http://fly.bio.indiana.edu/gal4.htm. pumpless-(ppl)-GAL4 is described in Zinke et al. (1999). Lsp2-Gal4 was provided by B. Hassan.

PIP Binding Assay

Bacteria expressing HIS-tagged Melted were lysed by a freeze/thaw cycle, subsequent addition of 0.2 mg/ml lysozyme and 0.2 mg/ml DNase, incubation on ice for 30 min, and vigorous vortexing. No detergent was used because it inhibits binding to phosphoinositides. The lysate was cleared by centrifugation, diluted 1:1000 or 1:10,000 in TBST (10 mM Tris/HCl [pH 8.0], 150 mM NaCl, 0.1% Tween 20) + 3% BSA (fatty-acid free) + protease inhibitors, and incubated for 1 hr with PIP membranes (Echelon Biosciences) preblocked with 3% fatty-acid-free BSA in TBST. Strips were washed twice with TBST for 30 min, incubated for 1 hr room temperature with anti-HIS in TBST + 3% BSA followed by HRP-conjugated 2° antibody.

Y2H

A *Drosophila* larval-cDNA library in pGAD-C was kindly provided by Grace Gill. The yeast two-hybrid screen was carried out in the strain PJ69-4a, containing reporters for lacZ expression and for growth on adenine and histidine. PJ69-4 a(*ura3*$^-$, *leu2*$^-$) was transformed with pAT165. Melt expression was verified by immunoblotting. This was transformed with library plasmid DNA and plated on ura$^-$leu$^-$ade$^-$ dropout synthetic medium to select for presence of the bait plasmid (URA3), the library plasmid (LEU2), and for activation of the adenine reporter. Colonies were retested for growth on ura$^-$leu$^-$ade$^-$his$^-$ medium for activation of the histidine reporter and on X-gal plates. Plasmids were isolated from clones that satisfied all these reporter-construct requirements. Sequences also identified in a second independent screen were considered nonspecific and discarded.

Antibodies

Anti-dMelt was raised in rats against the full-length protein expressed in *E. coli*. Rats were injected with 50 μg dMelt protein in RIBI adjuvent. For immunoprecipitation, cells were lysed for 5–10 min on ice in 50 mM Tris (pH 7.5), 150 mM NaCl, 1% Triton X-100 (with protease and phosphatase inhibitors). Lysates were cleared by centrifugation at 4°C at maximum speed for 15 min and incubated with antibody for 2 hr at 4°C. 50 μl of 50% agarose-protein A bead slurry was washed twice in lysis buffer and added to the antibody/cell-lysate mixture for 30 min. After three washes with cold lysis buffer, proteins were recovered with 2× protein-gel loading buffer and heating for 5 min at 95°C.

Fly Measurement and Metabolic Characterization

Metabolic measurements were done on test and control flies grown under identical conditions. 50 newly hatched first instar larvae were seeded per vial and adults hatching on the same day were aged for 2 or 3 days before testing. Male flies were weighed in batches of 50. Total body triglycerides were measured by homogenizing flies in 0.05% Tween 20 with protease inhibitors. After heating at 70°C for 5 min, lysates were cleared by centrifugation and triglycerides measured with Infinity Triglyerides Reagent (Thermoelectron). Total protein was measured on the same samples by Biorad protein assay. 1 μl of hemolymph was put into 9 μl of buffer (5 mM Tris [pH 6.6], 137 mM NaCl, 2.7 mM KCl), heated for 5 min at 70°C, incubated with 1 μl of porcine trehalase (Sigma T-8778) at 37°C for 12 hr, and measured with Sigma glucose (G) assay kit (GAGO-20) to measure sugars.

Microarray Analysis

Fat bodies from ten male, wandering third instar larvae of each genotype were dissected, and RNA extracted by a standard TRIzol (Invitrogen) procedure. RNA was reverse transcribed and linearly amplified by the SMART protocol (BD Biosciences). cDNA was directly labeled with the BioPrime array CGH labeling system (Invitrogen) and hybridized to microarrays containing the DGC1 and DGC2 collections. Two technical replicates were performed, and the whole experiment repeated twice on two biological replicates.

Supplemental Data

Supplemental Data include one table and can be found with this article online at http://www.developmentalcell.com/cgi/content/full/9/2/271/C1/.

Acknowledgments

We thank Thomas Sandmann and the European Molecular Biology Laboratory Genecore for help with microarrays; Julius Brennecke for the deletion mutants; Ernst Hafen, Bassem Hassan, and D.J. Pan for sharing reagents; and Ann-Mari Voie and Silke Eckert for technical assistance. A.T. was supported by a Howard Hughes Medical Institute PhD fellowship.

Received: February 23, 2005
Revised: May 18, 2005
Accepted: July 13, 2005
Published: August 2, 2005

References

Accili, D., and Arden, K.C. (2004). FoxOs at the crossroads of cellular metabolism, differentiation, and transformation. Cell *117*, 421–426.

Arquier, N., Bourouis, M., Colombani, J., and Leopold, P. (2005). Drosophila Lk6 kinase controls phosphorylation of eukaryotic translation initiation factor 4E and promotes normal growth and development. Curr. Biol. *15*, 19–23.

Baker, J., Liu, J.P., Robertson, E.J., and Efstratiadis, A. (1993). Role of insulin-like growth factors in embryonic and postnatal growth. Cell *75*, 73–82.

Bšhni, R., Riesgo-Escovar, J., Oldham, S., Brogiolo, W., Stocker, H., Andruss, B.F., Beckingham, K., and Hafen, E. (1999). Autonomous control of cell and organ size by CHICO, a drosophila homolog of vertebrate IRS1-4. Cell *97*, 865–875.

Britton, J.S., Lockwood, W.K., Li, L., Cohen, S.M., and Edgar, B.A. (2002). *Drosophila*'s insulin/PI3-kinase pathway coordinates cellular metabolism with nutritional conditions. Dev. Cell *2*, 239–249.

Brogiolo, W., Stocker, H., Ikeya, T., Rintelen, F., Fernandez, R., and Hafen, E. (2001). An evolutionarily conserved function of the *Drosophila* insulin receptor and insulin-like peptides in growth control. Curr. Biol. *11*, 213–221.

Brugarolas, J., Lei, K., Hurley, R.L., Manning, B.D., Reiling, J.H., Hafen, E., Witters, L.A., Ellisen, L.W., and Kaelin, W.G., Jr. (2004). Regulation of mTOR function in response to hypoxia by REDD1 and the TSC1/TSC2 tumor suppressor complex. Genes Dev. *18*, 2893–2904.

Brunet, A., Bonni, A., Zigmond, M.J., Lin, M.Z., Juo, P., Hu, L.S., Anderson, M.J., Arden, K.C., Blenis, J., and Greenberg, M.E. (1999). Akt promotes cell survival by phosphorylating and inhibiting a Forkhead transcription factor. Cell *96*, 857–868.

Canavoso, L.E., Jouni, Z.E., Karnas, K.J., Pennington, J.E., and Wells, M.A. (2001). Fat metabolism in insects. Annu. Rev. Nutr. *21*, 23–46.

Cho, H., Mu, J., Kim, J.K., Thorvaldsen, J.L., Chu, Q., Crenshaw, E.B., 3rd, Kaestner, K.H., Bartolomei, M.S., Shulman, G.I., and Birnbaum, M.J. (2001). Insulin resistance and a diabetes mellitus-like syndrome in mice lacking the protein kinase Akt2 (PKBbeta). Science *292*, 1728–1731.

Dong, J., and Pan, D. (2004). Tsc2 is not a critical target of Akt during normal *Drosophila* development. Genes Dev. *18*, 2479–2484.

Duchek, P., Somogyi, K., Jekely, G., Beccari, S., and Rorth, P. (2001). Guidance of cell migration by the Drosophila PDGF/VEGF receptor. Cell *107*, 17–26.

Gao, X., and Pan, D. (2001). TSC1 and TSC2 tumor suppressors antagonize insulin signaling in cell growth. Genes Dev. *15*, 1383–1392.

George, S., Rochford, J.J., Wolfrum, C., Gray, S.L., Schinner, S., Wilson, J.C., Soos, M.A., Murgatroyd, P.R., Williams, R.M., Acerini, C.L., et al. (2004). A family with severe insulin resistance and diabetes due to a mutation in AKT2. Science *304*, 1325–1328.

Hachet, O., and Ephrussi, A. (2001). *Drosophila* Y14 shuttles to the posterior of the oocyte and is required for oskar mRNA transport. Curr. Biol. *11*, 1666–1674.

Hafen, E. (2004). Interplay between growth factor and nutrient signaling: lessons from *Drosophila* TOR. Curr. Top. Microbiol. Immunol. *279*, 153–167.

Hanson, R.W., and Reshef, L. (2003). Glyceroneogenesis revisited. Biochimie *85*, 1199–1205.

Hay, N., and Sonenberg, N. (2004). Upstream and downstream of mTOR. Genes Dev. *18*, 1926–1945.

Hennig, K.M., and Neufeld, T.P. (2002). Inhibition of cellular growth and proliferation by dTOR overexpression in *Drosophila*. Genesis *34*, 107–110.

Hwangbo, D.S., Gersham, B., Tu, M.P., Palmer, M., and Tatar, M. (2004). *Drosophila* dFOXO controls lifespan and regulates insulin signalling in brain and fat body. Nature *429*, 562–566.

Ikeya, T., Galic, M., Belawat, P., Nairz, K., and Hafen, E. (2002). Nutrient-dependent expression of insulin-like peptides from neuroendocrine cells in the CNS contributes to growth regulation in *Drosophila*. Curr. Biol. *12*, 1293–1300.

Inoki, K., Zhu, T., and Guan, K.L. (2003). TSC2 mediates cellular energy response to control cell growth and survival. Cell *115*, 577–590.

Junger, M.A., Rintelen, F., Stocker, H., Wasserman, J.D., Vegh, M., Radimerski, T., Greenberg, M.E., and Hafen, E. (2003). The *Drosophila* forkhead transcription factor FOXO mediates the reduction in cell number associated with reduced insulin signaling. J. Biol. *2*, 20.

Kops, G.J., de Ruiter, N.D., De Vries-Smits, A.M., Powell, D.R., Bos, J.L., and Burgering, B.M. (1999). Direct control of the Forkhead transcription factor AFX byprotein kinase B. Nature *398*, 630–634.

Kwiatkowski, D.J. (2003). Tuberous sclerosis: from tubers to mTOR. Ann. Hum. Genet. *67*, 87–96.

Lee, G., and Park, J.H. (2004). Hemolymph sugar homeostasis and starvation-induced hyperactivity affected by genetic manipulations of the adipokinetic hormone-encoding gene in *Drosophila melanogaster*. Genetics *167*, 311–323.

Lee, Y.S., and Carthew, R.W. (2003). Making a better RNAi vector for *Drosophila*: use of intron spacers. Methods *30*, 322–329.

Miron, M., Verdu, J., Lachance, P.E., Birnbaum, M.J., Lasko, P.F., and Sonenberg, N. (2001). The translational inhibitor 4E-BP is an effector of PI(3)K/Akt signalling and cell growth in *Drosophila*. Nat. Cell Biol. *3*, 596–601.

Muto, E., Tabata, Y., Taneda, T., Aoki, Y., Muto, A., Arai, K., and Watanabe, S. (2004). Identification and characterization of Veph, a novel gene encoding a PH domain-containing protein expressed in the developing central nervous system of vertebrates. Biochimie *86*, 523–531.

Potter, C.J., Huang, H., and Xu, T. (2001). *Drosophila* Tsc1 functions with Tsc2 to antagonize insulin signaling in regulating cell growth, cell proliferation, and organ size. Cell *105*, 357–368.

Preston, C.R., and Engels, W.R. (1996). P-element-induced male recombination and gene conversion in *Drosophila*. Genetics *144*, 1611–1622.

Puig, O., Marr, M.T., Ruhf, M.L., and Tjian, R. (2003). Control of cell number by *Drosophila* FOXO: downstream and feedback regulation of the insulin receptor pathway. Genes Dev. *17*, 2006–2020.

Reiling, J.H., and Hafen, E. (2004). The hypoxia-induced paralogs Scylla and Charybdis inhibit growth by down-regulating S6K activity upstream of TSC in *Drosophila*. Genes Dev. *18*, 2879–2892.

Reiling, J.H., Doepfner, K.T., Hafen, E., and Stocker, H. (2005). Diet-dependent effects of the *Drosophila* Mnk1/Mnk2 homolog Lk6 on growth via eIF4E. Curr. Biol. *15*, 24–30.

Rusten, T.E., Lindmo, K., Juhasz, G., Sass, M., Seglen, P.O., Brech, A., and Stenmark, H. (2004). Programmed autophagy in the *Drosophila* fat body is induced by ecdysone through regulation of the PI3K pathway. Dev. Cell *7*, 179–192.

Sandri, M., Sandri, C., Gilbert, A., Skurk, C., Calabria, E., Picard, A., Walsh, K., Schiaffino, S., Lecker, S.H., and Goldberg, A.L. (2004). Foxo transcription factors induce the atrophy-related ubiquitin ligase atrogin-1 and cause skeletal muscle atrophy. Cell *117*, 399–412.

Saucedo, L.J., Gao, X., Chiarelli, D.A., Li, L., Pan, D., and Edgar, B.A. (2003). Rheb promotes cell growth as a component of the insulin/TOR signalling network. Nat. Cell Biol. *5*, 566–571.

Stocker, H., Radimerski, T., Schindelholz, B., Wittwer, F., Belawat, P., Daram, P., Breuer, S., Thomas, G., and Hafen, E. (2003). Rheb is an essential regulator of S6K in controlling cell growth in *Drosophila*. Nat. Cell Biol. *5*, 559–565.

Tapon, N., Ito, N., Dickson, B.J., Treisman, J.E., and Hariharan, I.K. (2001). The *Drosophila* tuberous sclerosis complex gene homologs restrict cell growth and cell proliferation. Cell *105*, 345–355.

Teleman, A.A., Chen, Y.-W., and Cohen, S.M. (2005). 4E-BP functions as a metabolic brake used under stress conditions but not during normal growth. Genes Dev., in press.

Tettweiler, G., Miron, M., Jenkins, M., Sonenberg, N., and Lasko, P.F. (2005). Starvation and oxidative stress resistance in *Drosophila* are mediated through the eIF4E-binding protein, d4E-BP. Genes Dev., in press.

Tsukiyama-Kohara, K., Poulin, F., Kohara, M., DeMaria, C.T., Cheng, A., Wu, Z., Gingras, A.C., Katsume, A., Elchebly, M., Spiegelman, B.M., et al. (2001). Adipose tissue reduction in mice lacking the translational inhibitor 4E-BP1. Nat. Med. *7*, 1128–1132.

Tusher, V.G., Tibshirani, R., and Chu, G. (2001). Significance analysis of microarrays applied to the ionizing radiation response. Proc. Natl. Acad. Sci. USA *98*, 5116–5121.

Um, S.H., Frigerio, F., Watanabe, M., Picard, F., Joaquin, M., Sticker, M., Fumagalli, S., Allegrini, P.R., Kozma, S.C., Auwerx, J., and Thomas, G. (2004). Absence of S6K1protects against age- and diet-induced obesity while enhancing insulin sensitivity. Nature *431*, 200–205.

Withers, D.J., Gutierrez, J.S., Towery, H., Burks, D.J., Ren, J.M., Previs, S., Zhang, Y., Bernal, D., Pons, S., Shulman, G.I., et al. (1998). Disruption of IRS-2 causes type 2 diabetes in mice. Nature *391*, 900–904.

Wolfrum, C., Besser, D., Luca, E., and Stoffel, M. (2003). Insulin regulates the activity of forkhead transcription factor Hnf-3beta/Foxa-2 by Akt-mediated phosphorylation and nuclear/cytosolic localization. Proc. Natl. Acad. Sci. USA *100*, 11624–11629.

Zhang, Y., Gao, X., Saucedo, L.J., Ru, B., Edgar, B.A., and Pan, D. (2003). Rheb is a direct target of the tuberous sclerosis tumour suppressor proteins. Nat. Cell Biol. *5*, 578–581.

Zimmermann, R., Strauss, J.G., Haemmerle, G., Schoiswohl, G., Birner-Gruenberger, R., Riederer, M., Lass, A., Neuberger, G., Eisenhaber, F., Hermetter, A., and Zechner, R. (2004). Fat mobilization in adipose tissue is promoted by adipose triglyceride lipase. Science *306*, 1383–1386.

Zinke, I., Kirchner, C., Chao, L.C., Tetzlaff, M.T., and Pankratz, M.J. (1999). Suppression of food intake and growth by amino acids in *Drosophila*: the role of pumpless, a fatbody expressed gene with homology to vertebrate glycine cleavage system. Development *126*, 5275–5284.

Zinke, I., Schutz, C.S., Katzenberger, J.D., Bauer, M., and Pankratz, M.J. (2002). Nutrient control of gene expression in *Drosophila*: microarray analysis of starvation and sugar-dependent response. EMBO J. *21*, 6162–6173.